12

The injector with thermionic gridded cathode radiofrequency gun for the SKIF synchrotron

© V.N. Volkov,[1] M.V. Arsentieva,[1,2,3] A.M. Barnyakov,[1] A.M. Batrakov,[1] E.A. Bekhtenev,[1] N.G. Vasileva,[1] S.M. Gurov,[1] S.E. Karnaev,[1] A.A. Kondakov,[1] A.N. Kosarev,[1] S.A. Krutikhin,[1] G.Ya. Kurkin,[1] A.E. Levichev,[1,2,3] A.Yu. Martynovskiy,[1] O.I. Meshkov,[1,2] S.V. Motygin,[1] D.A. Nikiforov,[1,3] V.K. Ovchar,[1] A.V. Pavlenko,[1] O.A. Pavlov,[1] M.V. Rodyakin,[1] E.A. Rotov,[1] I.K. Sedlyarov,[1] A.M. Semenov,[1,2,5] X.C. Ma,[1,4] M.G. Fedotov[1]

[1] Budker Institute of Nuclear Physics, Siberian Branch, Russian Academy of Sciences, Novosibirsk, Russia
[2] Novosibirsk State University, Novosibirsk, Russia
[3] SRF „SKIF“, Nikolsky Av., 630559 Kol'tsovo, Russia
[4] National Synchrotron Radiation Laboratory (NSRL), USTC, China
[5] Novosibirsk State Technical University, Novosibirsk, Russia
e-mail: V.N.Volkov@inp.nsk.su

Received February 8, 2024 Revised April 5, 2024 Accepted April 18, 2024

Budker Institute of Nuclear Physics (BINP) is carrying out work with SKIF synchrotron of fourth generation. Synchrotron buildings are reared now in the ground of Koltcovo. In BINP there is the stand for testing of first part of SKIF injector (preinjector) that includes gridded thermionic cathode radiofrequency (RF) gun which is applying for the first time in world practice. The main goal of the pre-injector is the forming of short electron bunches with low energy spread and the accelerating up to relativistic energies. In the article the preinjector structure, principle of operation and tuning are described. Specific features related with RF gun applying are checked. Numerically calculated and measured beam characteristics in the preinjector are analyzed. Methods of preinjector characteristic calibration and tuning are discussed.

Keywords: Bunching RF system, Longitudinal bunching dynamics, Bunch duration, Energy spread.

DOI: 10.61011/TP.2024.06.58827.32-24

Introduction

In contrast to a SKIF injector [1] with a high-frequency (RF) gun, most synchrotrons use static guns with a thermionic cathode controlled with the help of a grid. In such guns the voltage pulse with duration of 1−2 ns on the cathode unlocks the electron beam from the cathode, which, passing through the grid, accelerates in the electrostatic field of the gun to relatively low energy of 50−100 keV. Further the obtained bunches pass through RF fields of buncher cavities and shortening in length to tens of picoseconds to enable their further acceleration to energy of 3−4 MeV in a preliminary accelerator 2856 MHz and further in a linear accelerator 2856 MHz to energy of 100−200 MeV. In injectors it is necessary to obtain beam energy spread of at least 1%. This principle of operation is used by injectors of DLS [2], SLS [3], NSLS [4], ESRF [5], ALS [6] and many other synchrotrons. The same principle is used in the described SKIF injector [7], only instead of a static gun first time in the global practice a thermionic cathode grid-controlled RF gun is used [8].

A disadvantage of electrostatic guns is low beam energy, presence of ionic bombardment of the cathode from the gas molecules positively ionized in vacuum and the need to use a bulky high voltage equipment, which is dangerous and inconvenient to operate. Such guns have higher requirements to vacuum and, moreover, requirements to reducing the longitudinal dimensions of the entire injector to decrease the grouping time, when the beam emittance deteriorates fast because of relatively low energy under impact of its spatial charge.

RF guns have no such disadvantages. In the RF field ionic bombardment is almost absent, since massive ions have no time to speed up in the RF field to the energies that may damage the cathode. As a result of this the problem of the cathode lifetime becomes irrelevant (not taking into account the ageing), and requirements to vacuum in the injector are substantially less strict [9,10]. A thermionic cathode with grid control, principally the same as in ordinary static guns, is placed in the RF field in the rear wall of a special RF cavity. Then downstream the RF gun the beam is grouped using the same principle as in injectors with static guns, and is then accelerated first in the preliminary accelerator and then in a linear accelerator 2856 MHz up to 200 MeV.

The value of the RF gun accelerating voltage is not limited by development of the ionic back bombardment effect, as in static guns, therefore RF voltage and beam energy of the RF gun may be increased up to 1 MeV. As a result of that the drift space of the preinjector bunches grouping extends to 2−3 m, and the necessary diagnostic equipment is freely located thereon. Therefore, use of the RF gun in the injector of the fourth generation synchrotron SKIF simplifies and cheapens its design and operation, and improves the quality of the electron beam. Two similar (but not pulse) RF guns created in the Institute of Nuclear Physics [9,10], in practice confirm the above properties. Photocathode RF guns with a complex laser

system, especially superconducting ones, are not considered here since so far both quite reliable photocathodes have not been designed yet for them, as well as the cheap technology of RF superconductivity. Further descriptions of other thermionic cathode RF guns used in the global practice are provided for comparison.

RF guns 2856 MHz with a thermionic cathode and without a control grid are world-wide, where the cathode is installed on the rear wall of the RF cavity [11]. Electrons are emitted from the cathode during the positive RF half-period, and relatively long bunches produced in this manner are accelerated in the RF field. Then bunches are grouped in a special rotary α-magnet. By cost and complexity the injectors of such design are practically the same as the above injector with static guns [12]. Their disadvantage is the presence of back accelerated electrons that bombard the cathode and decrease its lifetime, and difficulties with obtaining single electron bunches.

Thermionic cathode RF guns with a built-in grid (without external control), which are used in powerful industrial ILA amplifiers, do not have such disadvantages [13]. Electrons from the cathode are emitted by RF field of the gun, penetrating through the grid during the positive half-period of RF field. Owing to voltage induced by the beam on the grid, the emission of the electron bunch from the cathode is interrupted at the phase of RF field, after which the emitted electrons are slowed down in the alternating RF field that changed its sign and are accelerated in the opposite direction, bombarding the cathode (as it happens in the RF guns without a grid). The grid here is controlled by voltage pulses induced by the bunch itself in the capacitance of cathode–grid, phase-shifted by a special short-circuiting coaxial loop of a certain length. Besides, permanent bias offset is additionally supplied to the cathode via the loop, which also controls the emission duration. The average current of the beam in these amplifiers — 0.5–1.5 A, and the cathode life time — up to 2000 h, which clearly demonstrates the advantage of RF guns vs static guns. Such RF guns generate only a series of bunches.

1. Structure and parameters of SKIF preinjector

The preinjector (Fig. 1) comprises: modulator of cathode-grid unit *1*, RF gun 178.5 MHz *2*, buncher cavity 535.5 MHz *5*, preliminary accelerator on a traveling wave 2856 MHz *10* and the first of five multi-cell accelerating sections on a traveling vave with accelerating mode $2\pi/3$ *11*. For RF supply, the injector uses two impulse solid-state amplifiers for 178.5 MHz (700 kW) and 535.5 MHz (10 kW), and also one of three klystrons 2856 MHz (40 MW) with a derivation of RF capacity of 10 MW for a preliminary accelerator. A standard system of control and synchronization from Libera is used. The RF gun generates electron bunches with energy of up to 700 keV and repetition frequency of 1 Hz in two modes: single bunches 1 nC, or a series of 55 bunches of 0.3 nC, or any other combination of bunches with a total charge of not more than 16 nC. (Time to tune/switch operation of the injector from one mode to another is approximately half an hour, if the method is finalized.) Bunches are grouped in the preinjector from 1 ns to 6–10 ps (FWHM) as they accelerate to energy of 2–3 MeV in the preinjector and accelerate further to 30–45 MeV in the accelerating section. The injector must provide the energy spread of bunches not exceeding 1% (rms (root mean square)), time instability of below 2 ps, normalized emittance of at least 60π mm·mrad and energy of 200 MeV.

2. Dynamics of electron bunch in preinjector

The source of electrons in the RF gun is a thermionic cathode, controlled in the gap of cathode–grid by pulse voltage with amplitude of up to 100 V with duration of 1 ns. The purpose of the preinjector is a longitudinal grouping of nanosecond electron bunches from the RF gun to the duration of less than 10 ps with energy spread of up to 1% (rms). This is achieved by creating the corresponding distribution of the charge density and energy of particles along the bunches. The principle of longitudinal grouping of bunches in the RF gun and in the preinjector consists in developing higher speed of particles in the tail portion of the bunch, because of which the electrons in this part of the bunch catch up with the particles in the front edge of the bunch in a certain drift space. Then after acceleration of the grouped bunch to relativistic energies, grouping stops. Bunches from the RF gun have nonuniform longitudinal distribution of energy already, which follows the sine dependence of voltage on the RF gun and contributes to the grouping effect. Solving a simple exercise on the distance, at which the second particle catches up with the first one, if its energy is higher than that of the first one at this dependence, is expressed as follows:

$$S = \frac{c}{\omega}\sqrt{(E/mc^2+2)^3 \cdot E/mc^2}\cdot tg(\varphi), \qquad (1)$$

where E — maximum energy of particles (or RF voltage amplitude in [eV]), ω — RF circular frequency in the gun, φ — RF phase, at which particles are emitted, c — light velocity, m — electron mass.

The curve of dependence (1) is shown in Fig. 2, *a*. From the curve one may see that for RF voltages of 700–800 kV the length of the drift gap is around 2 m. This gap determines the dimensions of the grouping area. For comparison, most static guns with beam energy of 50–100 keV and the corresponding voltage of the buncher cavity $\sim$ 50 kV this gap is only 20 cm.

The similar analysis shows that the grouping effect also occurs in the cathode–grid gap, where the trigger voltage also varies following the sinusoidal law with equivalent

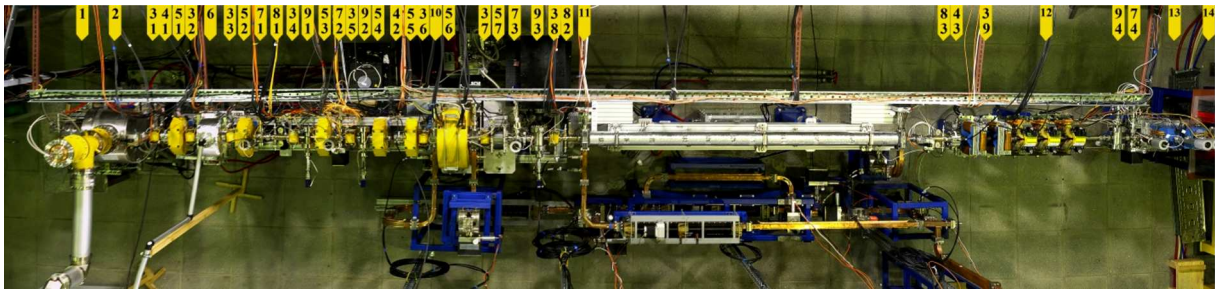

Figure 1. Preinjector of SKIF accelerator: *1* — modulator (inside the RF gun); *2* — RF gun, *3/1–3/9* — correctors; *4/1–4/3* — FCT sensors s(Fast Current Transformer); *5/1–5/7* — solenoids; *6* — buncher cavity 535.5 MHz; *7/1–7/4* — luminophores; *8/1–8/3* — pickups; *9/1–9/4* — streak cameras; *10* — preinjector (inside the solenoid *5/6*); *11* — accelerating section 2856 MHz; *12* — triplet; *13* — scanner; *14* — Faraday cylinder.

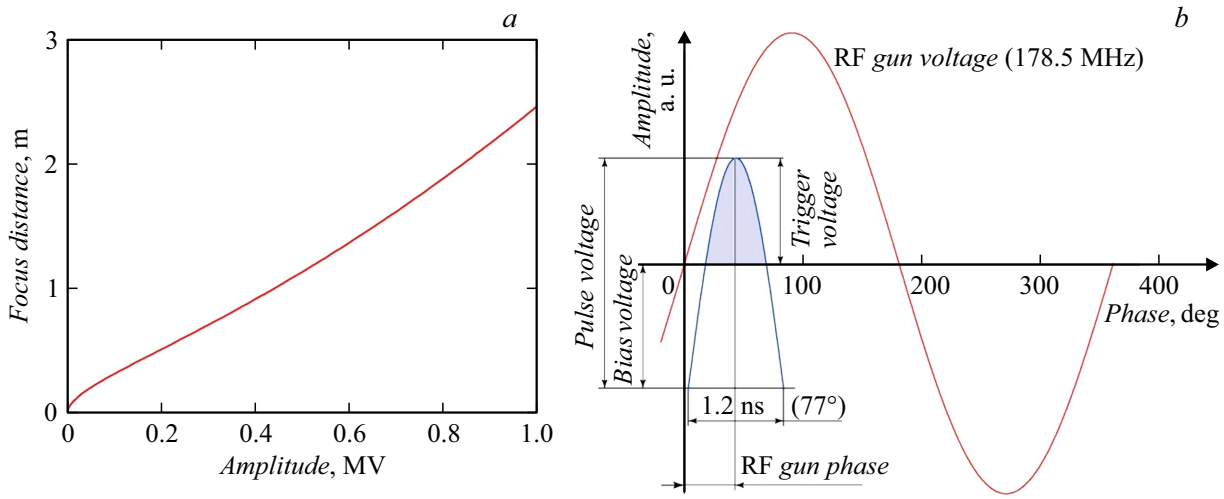

Figure 2. Bunch grouping effect: *a* — dependence of the focus distance of longitudinal grouping on the cavity voltage amplitude (see (1) at $\varphi = 45°$), *b* — voltage shapes in the RF gun: *Pulse Voltage* — voltage pulse amplitude, *Bias Voltage* — bias offset, *Trigger Voltage* — trigger voltage.

frequency 400 MHz and with amplitude around 50 V (Fig. 2, *b*). According to equation (1), this cathode grouping occurs at the distance 2–6 mm from the cathode. Calculations predict formation of a steep front in the longitudinal distribution of bunch charge. Calculations also predict (with account of the effect of the spike in current in the area free of electrons upstream the cathode, where at the initial triggering moment the Langmuir 3/2 law does not work), that the peak current of the cathode at the front edge of bunches may exceed the emission current dozens of times.

During further analysis of the grouping processes it is taken into account that the principle of maintaining the transverse emittance, according to the Liouville's theorem, here, in the grouping section, may not be applied because of a relatively long lengths and energy spread of nonrelativistic bunches [12], since different parts of the long bunch are accelerated and focused by the alternating RF field differently. Besides, the mentioned known law 3/2 is not applicable when calculating the current of emission from the cathode, as it is made for the stationary conditions of an infinitely long beam. Here, in fast-alternating RF fields, numerical modeling of electron beam is used, which takes into account the inertial dynamics of electron motion.

When developing the numerical model of the preinjector, ASTRA [14] package was widely used, where the interaction of the electron beam with RF fields and between each other is modelled by their equivalent macroparticles. Besides, electronic bunches are represented in the form of array of several dozens of thousands of macroparticles. Numerical models of bunch dynamics in the cathode-grid unit [15], and also distribution of electromagnetic fields in cavities of RF gun, buncher and accelerating cavities, were created using software suites SLANS, CLANS, SAM [16] and CST [17].

Electronic beam calculations were carried out sequentially in all parts of the preinjector, starting from the cathode-grid unit with longitudinal dimensions of the order of 80 μm. Then follows the accelerating gap of the RF gun with size

of 80 mm and grouping and acceleration with total length of 8 m (fig. 1).

The origin in all calculations is the center of the cathode, the position of which is controlled by the system of geographical indicators on the body of the RF gun. For further analysis it is necessary to determine the concept of the phase of RF field not only in RF gun, but in all cavities of the injector and the entire synchrotron. An RF phase is generally called the phase of RF voltage in any cavity that is in effect at the moment of escape of the central part of the bunch from the cathode (fig. 2, *b*). Let us emphasize that these are not those RF phases, which operate in the cavities in the moment of bunches flying through them.

In the numerical model of the cathode-grid unit, continuous emission of charged macroparticles is carried out with emission current of 2.0 A and energy of 0.1−0.5 eV. They develop electric field of space charge directed against movement. Because of this some emitted particles return to the cathode, and some of them, depending on the applied voltage, reach the grid and either settle on it, or fly through cells and the grid outside, into the cavity of the RF gun — as it happens in the real case with electrons. A voltage pulse from the modulator arriving to the gap of cathode−grid is modelled in the shape of the half cosine wave with width at the base 1.2 ns (400 MHz) and amplitude 100 V (Fig. 2, *b*). Besides, constant bias voltage 0−100 V is applied to the gap. The difference between one and the other is trigger voltage. Electric fields from these voltages and RF field penetrating through the grid from the cavity, and also fields of the space charge are summed up in the gap according to the superposition principle.

Upon impact of this combination of electric fields at each charged particle emitted from the cathode, a beam is formed as a bunch with duration of less then 1 ns, which, reaching the accelerating phase of RF voltage in the cavity is accelerated by its RF field. Since each of particles in the bunch gets into its determined RF phase in the cavity, at the outlet from the cavity the particles receive each their certain energy, therefore the bunch from the RF gun has a specific non-linear longitudinal distribution of particle energies close to harmonic dependence. This distribution depends on RF phase, which was present at the moment of gate impulse middle arrival. Fig 3, *a* shows these estimated distributions for three different RF phases in the gun — 30°, 50° and 70°.

The value of the bunch charge and its length are formed by the top of the voltage pulse determined by the difference of its amplitude and the value of the bias offset (Fig. 2, *b*). The least short bunches are produced at the maximum amplitude of the voltage pulse, i. e. at its shortest top. Because of this the amplitude of this impulse is fixed by 100 V, and the charge is controlled by the bias offset. Thus, charge of 0.3 nC is produced by bias offset 100 V mostly due to the electric RF field from the cavity penetrating through the grid. Besides, the estimated length of the bunch is 45 mm (FWHM). To generate charge of 1.2 nC in the bunch, bias offset 30 V is required, and the estimated length of the bunch is 138 mm, i. e. three times more.

Minimum turn-off bias must be 20 V, otherwise, in the idle mode, when there are no voltage pulses, dark current is emitted from the cathode by RF field penetrating through the grid in the form of bunches with charge of up to 0.3 nC and frequency of 178.5 MHz. Nevertheless, even with the cathode biased, there is dark current of several tens of μA observed from the RF gun, which is caused by autoemission of the grid and multipactor discharge on it. On the background of peak current of several amperes in the bunches, such dark current practically has no effect on beam quality.

For the injector the initial phases are important up to 55°, since distributions of particle energy at these phases contribute to grouping of bunches, when tail particles move faster than the front ones. The optimal phase in the SKIF injector is phase $\varphi = 40°$. At phases below 30° some head particles of bunches are cut, falling into negative phases of RF field. In phase 55° the particles in the beginning and in the end of the longitudinal distribution of bunch charge have the same energy, and the entire bunch in average has minimum energy spread. In this phase the bunches have maximum average energy $\sim 98\%$ of the amplitude voltage of the cavity. At phases higher than 55°, the particles in the front edge of the bunch have more energy and speed, compared to the tail, and the bunch elongates because of that in the drift space, and the bunch energy reduces.

Another specific phase is $\varphi = 90°$, when the bunch contains the maximum charge since at this phase the maximum RF field in the cavity is reached, which, penetrating to the cathode through the grid, pulls additional particles. This effect was used to calibrate RF phase by measured dependence of bunch charge on phase. At phases above 120° the particles in the tail portion of the bunches fail to fly till the end, since they are weakly accelerated by RF field that decreases after phase 90°. After the field sign changes ($\varphi > 180°$), these particles start accelerating in the opposite direction and reach the cathode with quite high energy, of the order of $1/2$ from the RF amplitude in the gun.

There are some effects related to impact of the grid at formation of bunches, not taken into account in the numerical model of the cathode-grid unit. The grid must partially screen the cathode from the electric field of the space charge of bunch having the length of the order of 50−150 mm. Calculations made with the inserted beam absorber behind the grid demonstrate that such screening results in charge growth in the bunches by 14% and reduction of time for particles flight in the cathode−grid gap by several degrees of RF phase in the cavity for bunches with charge of the order of 1 nC. Besides, here the axial asymmetry of halo beam is not taken into account as well, since the grid of the parquet type unit is presented by a model in the form of its equivalent axially symmetric grid made of 27 concentric rings [14]. Halo is caused by the edge effect from transverse focusing of the beam both on the edges of rectangular cells in the grid and the edges of

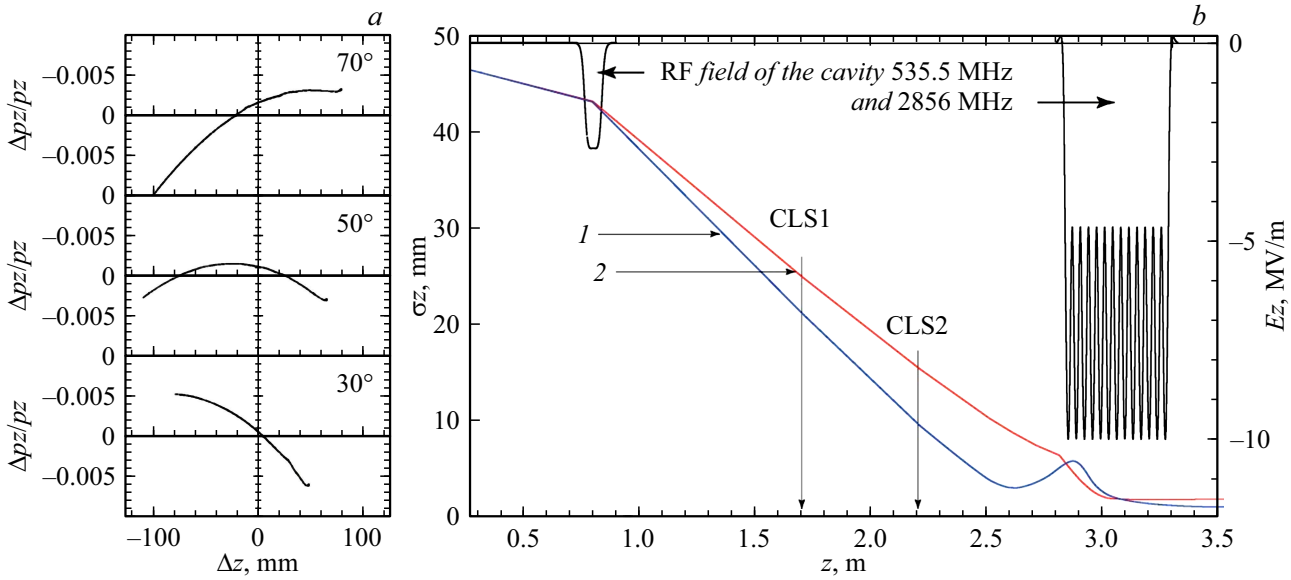

Figure 3. *a* — distribution of energy of particles along bunches depending on the phase of RF gun; *b* — change of rms length 1 nC of bunches downstream the buncher cavity depending on their coordinate for the pair of optimal phases (535.5 MHz) and phase 40° in the RF gun (estimate).

the rings in the equivalent grid. Halo intensity must depend on the total length of edges in all holes of the grid. In the numerical model with the circular grid this length of edges turned out to be twice larger than in the real grid of parquet type. Besides, the bias voltage is not taken into account, which is induced by the beam itself in the capacitance of the cathode–grid gap (12 pF), shunted with resistance 50 Ω. It is suggested that the modulator will compensate this voltage fully.

The critical role in the grouping of bunches is played by the buncher cavity for the third harmonic (535.5 MHz), located in the injector right after the RF gun (*6* in Fig. 1). RF phase in this cavity is opted as close to the phase when the bunches flying through it cut off the maximum energy ($\sim$ 150 keV). If tuning is accurate, electromagnetic RF field of cavity with optimal phase and amplitude must linearize the energy spread in the bunch so that in the end of the drift space, right upstream the preliminary accelerator or inside of it, all particles are grouped into a bunch of minimum size 2–3 mm (rms).

Calculations demonstrate that there are pairs of optimal cavity phases 535.5 MHz, which differ from each other in a pair by 10–15°. One of them suggests maximum grouping of bunches in coordinate $\sim$ 200 mm upstream the preliminary accelerator, and the other one — inside of it. Fig. 3, *b* shows estimated variation of bunch lengths in the grouping area of the injector for one of such phase pairs. To determine the phase of the grouping cavity 535.5 MHz two Cherenkov sensors are used (CLS1, CLS2), located in coordinates 1.7 and 2.2 m. The first phase of the above pair must provide for the ratio of bunch lengths 2 ± 0.5 measured by streak cameras, and the second one — 1.5 ± 0.5.

Estimated dependences of length variation in coordinate 1.7 m for 0.3 nC bunches are given in Fig. 4, *a*. Fig. 4, *b* shows estimated ratios of bunch lengths in coordinates 1.7 and 2.2 m, where horizontal blurred lines indicate levels 1.5 and 2. Crossing of these levels with curves defines optimal phases of the buncher cavity 535.5 MHz. From Fig. 4 one may see how much the tuning parameters change depending on the phase of the RF gun, which means high requirements to stability and to accuracy of its phase setting.

As calculations and experiments demonstrate, it is possible to determine grouping modes for a wide range of amplitudes of RF voltages in RF cavities. In particular, modes 750 and 870 keV are researched in the RF gun, 100–200 keV in the buncher cavity, and also 1/3 of RF power from the nominal one in the preliminary accelerator and 1/2 of RF power in the accelerating section [18]. As a rule, it is always possible to find optimal values of phases in these RF devices providing for nominal grouping of bunches (10 ps). Hereinafter the set of precisely tuned phases means phases, deviation of which to a certain side causes linac exit bunch length or energy spread gaining in proportion to the squared phase deviation.

Therefore, the tuning of the preliminary injector is reduced to, at first, setting the phase in the RF gun 40°, then to setting one of two phases of the cavity 535.5 MHz in the pair, measured by streak cameras. Then the preliminary accelerator phase is tuned using minimum length of bunches at its output, measured there by a streak camera. Then the phase of the accelerating section is opted by maximum of bunch energy at its output or by minimum energy spread measured in the bend magnet of the scanner. Phases tuned in this manner are then confirmed by fine tuning within small limits ±(1–10°), based on the readings of

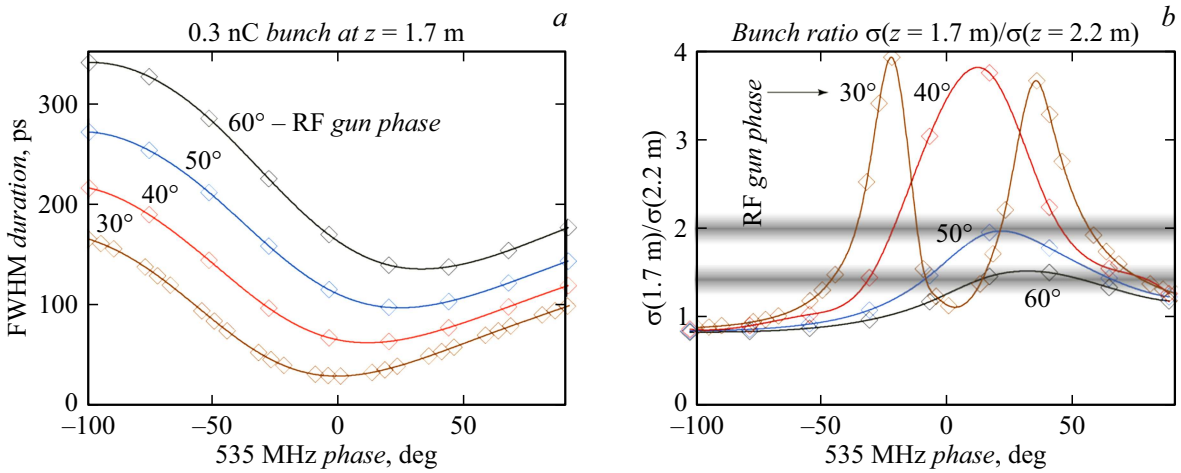

Figure 4. Estimated dependences on phases of RF cavities and phase 535 MHz: *a* — lengths of bunches in coordinate 1.7 m, *b* — ratio of lengths of these bunches in coordinates 1.7 and 2.2 m.

the streak camera at the output of the accelerating section or scanner in the bend magnet. Final phases of the preliminary accelerator and the accelerating section may be tuned simultaneously by changing the klystron phase.

As noted above, the tuned phases must be rather accurate and stable. Thus, the phase limits for all four RF devices of the preinjector, which provide the nominal energy spread of 1%, are shown for 0.3 nC bunches in Fig. 5 (inside dark bands). Calculations were made with account of potential losses of the bunch particles on the walls of the beam line with aperture 35 mm and on apertures in the preliminary accelerator and the accelerating section with diameter of 25.9 mm. In the curves one may see that beyond these bands all characteristics of bunches (energy spread, duration, emittance) start growing exponentially. Nevertheless, in all phase ranges on horizontal scales of curves the bunch travels without particle loss. This means that 100% passage of the bunch does not guarantee accurate tuning of the preinjector, since the energy rms spread at the same time may reach 20%, rms duration of bunches - 8 mm, emittance - 110π mm·mrad and energy drop - 20%.

It should be specifically emphasized how important it is to accurately set the phase of the RF gun, having the narrowest band of permissible phases 5–6°. Especially that for 1 nC bunches this band is two times narrower. Besides, the mode with series of 55 bunches (0.3 nCk) still requires additional research for stability, since its provision is related to features of modulator operation in multi-bunch mode.

It is noticed that the RF phase in the gun changes with time. Thus, for the summer period of vacations this phase changed by $\sim 50°$. After each switching of cables on the modulator blocks the phase goes to $\pm(1-20°)$. Therefore, it was decided to check the tuning of the RF gun phase every time prior to start of operation with the accelerator. For this purpose the automated calibration system is developed.

To achieve precision characteristics of the beam, it is necessary to provide high stability of RF supply characteristics in the accelerating cavities of the injector. For this purpose SKIF complex includes a system of frequency distribution, which generates and distributes within the complex a set of sinusoidal signals with frequencies 178.5, 357, 535.5, 2856 MHz with phase stability, including phase noise at the level of 2–4 ps. Measurements demonstrated the value of phase jitter in cavities of the RF gun and buncher cavity, and the beam jitter from two FCT sensors, around 5 ps from a peak to a peak (phase jitter $\Delta\varphi$ is related to time jitter $\Delta\tau$ as $\Delta\varphi = \omega\Delta\tau$, where ω — circular frequency of RF cavity). But this value also includes the added jitter of the measuring device, which is not known yet. For measurements the pulse shape and phase meter ADC4x250-FPM, was used, which receives the reference frequency signal 178.5 MHz as a timing one.

Stability of phases and amplitudes mainly depends on the stability of generators and quality of phase and amplitude systems of feedbacks regulating resonance frequencies of RF cavities and their RF amplitudes, and quality of RF cavities, preventing multipactor discharges and high voltage breakdowns. High quality of cavities was maintained by using the corresponding technology in their manufacturing and applying RF tests described in a separate article [19].

Section 3 considers methods of calibration of RF phases and voltages.

3. Calibration of phases and voltages of RF devices in preinjector

To improve accuracy of calibrations, the principle of averaging the maximum number of measurements was further used everywhere.

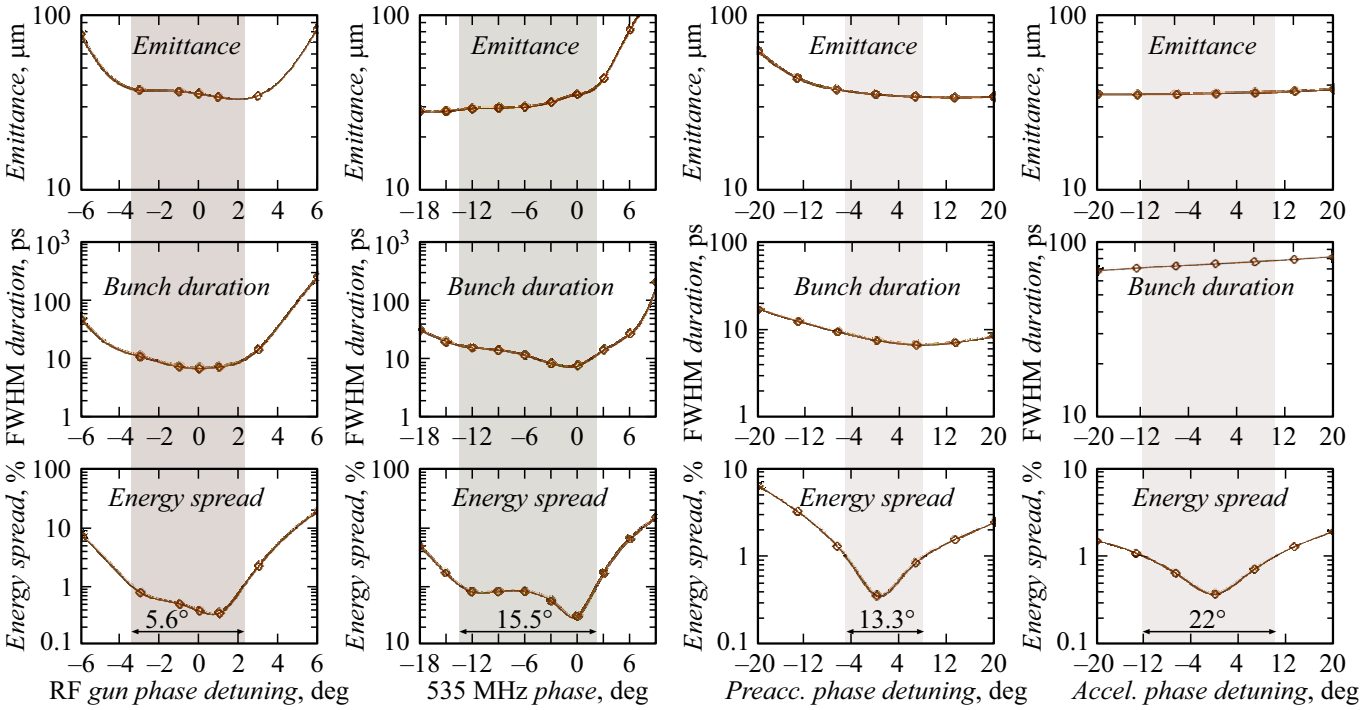

Figure 5. Dependence of parameters of 0.3 nC bunches at the output of the preinjector on shift of RF phases in RF devices of the preinjector.

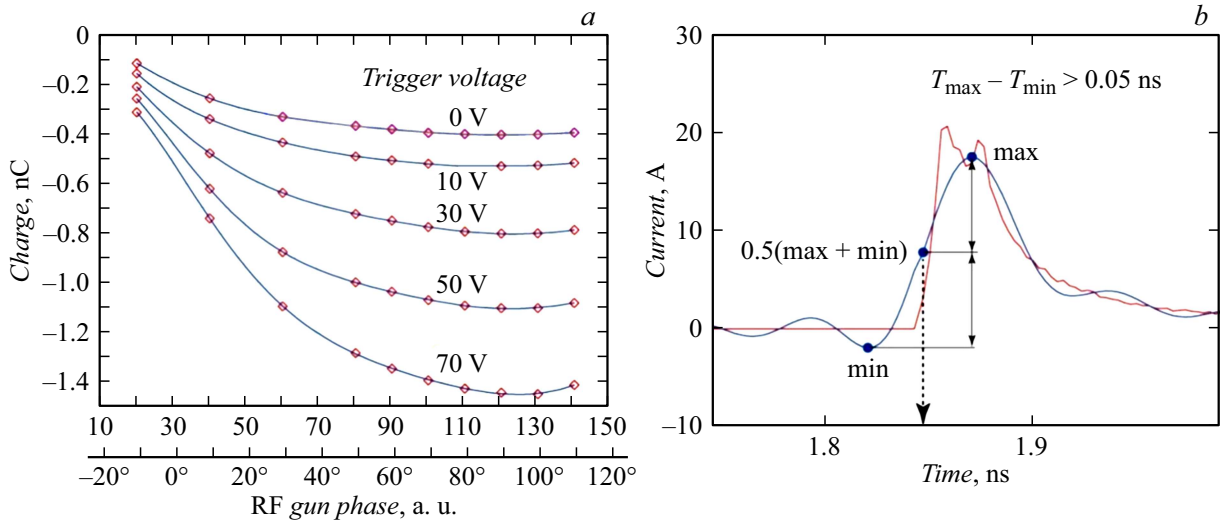

Figure 6. Calibration of RF gun phase by measurement (*a*) of dependences of the charge value on this phase and trigger voltage of the cathode by (*b*) integration of signals from FCT. Example of estimated distribution of current in the bunch (red) and its image (blue), obtained by limiting the spectrum with frequency of several GHz.

3.1. Calibration of RF gun phase

RF phase in the gun as defined above is a phase of RF voltage in the gun at the moment of emission of the bunch center from the cathode. This phase on the control panel is set by a conventional number, the value of which is proportionate to the phase in degrees, but is shifted by an uncertain value. During calibration, this conventional number is defined, corresponding to phase 90°, when the bunch charge is maximum due to maximum RF field penetrating from the cavity through the grid and emitting the charge from the cathode. For this purpose FCT (Fast Current Transformer) sensor measures several dependences of the charge values on the phase, differing by different values of cathode trigger voltages. Fig. 6, *a* shows an example of these measured dependences for trigger voltages of cathode 0, 10, 30, 50 and 70 V and new scale of phases in degrees produced as a result of calibration.

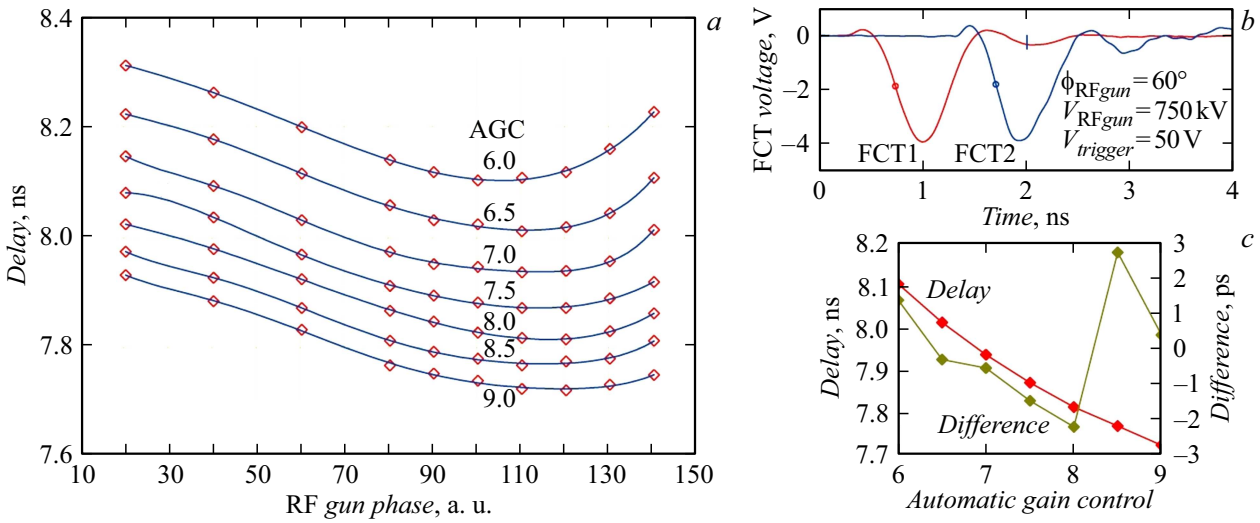

Figure 7. Measurements of dependence between delay of bunch passage (a), difference of minimum delays on theoretic dependence (b) and pulse view (FCT2 shifted by -7 ns) (c).

Table 1. Measured values of the phase set from a panel in charge maximum

Cathode trigger voltage, V	0	10	30	50	70
Reading on the panel at charge maximum	119.3	120.2	123.4	122.6	124.6
Rms spread of charge measurements, pC	1.02	0.46	0.79	1.19	2.18

These dependences are interpolated by sextic polynomial so that all measured points participate in calibration. Then in each dependence they define phases with maximum charge of bunches, and mean average of these phases is calculated. Table 1 shows the calibration results, from which the calculated value of the average value corresponding to phase 90°, is equal to 122.02 ± 1.98.

Charges in bunches were calculated by integration of curves of current distribution in bunches obtained in an oscilloscope by ROHDE-SCHWARZ from the FCT sensor. Fig. 6, b shows the typical appearance (Fig. 7, c) of such distribution indicated with a smooth (blue) curve. During integration, the negative values were taken into account in the form of the measured pulse, and the averaged curve was integrated by 10 pulses. Root-mean-square deviations of measured charge values from the interpolation curve given in Table 1 mean proper accuracy of these measurements.

Nevertheless, the resulting phases in the charge maximum for each curve differ strongly ($\pm 2°$). These differences of the curves may be explained by bias voltage induced by bunches that is proportionate to the charge value and not compensated fully by the modulator of the cathode and grid unit. Besides, the shape of curves depends on accelerating of electron beam intensity in the cathode–grid gap, specific for transition processes and depending on bias voltage [9]. It should be noted that the absolute value of RF gun phase 40° is not as critical for tuning of the preinjector grouping modes (for example, phases 38, 40, 42°), but its repetition is important every time during calibrations.

3.2. Voltage calibration in RF gun

Preliminary calibration of voltage in the RF gun was carried out using measured coupling coefficients of measuring loops, characteristics of RF gun cavity (Q factor, characteristic impedance) and measured input RF power from a directional coupler in the tract from the generator. Besides, inconsistences contributed when measuring characteristics of loops, RF gun and directional coupler. Most precise calibration was carried out by measuring the time of bunch passage between two FCT sensors. From the calculations it follows that the maximum energy of particles from the RF gun (at certain RF phase) is lower than voltage on the gun by $\sim 1\%$. Therefore, voltage on the RF gun may be measured with good precision by maximum energy of beam particles, specifically, the particles of the front edge of bunches. This energy was measured by time of passage between two FCT sensors with precision of 0.02%.

Measurements were carried out for some phases and some voltages on the RF gun (600–900 kV), which are set by the levels of the AGC — Automatic Gain Control system: AGC = 6, 6.5, 7, 7.5, 8, 8.5 and 9 (Fig. 7, a). These voltages ($\mathscr{E}$) are calculated using coefficient K ($\mathscr{E} = K \cdot \mathrm{AGG}$), which must be set by calibration.

From the obtained seven dependences of delays on the phase, the minimum values of delays were determined,

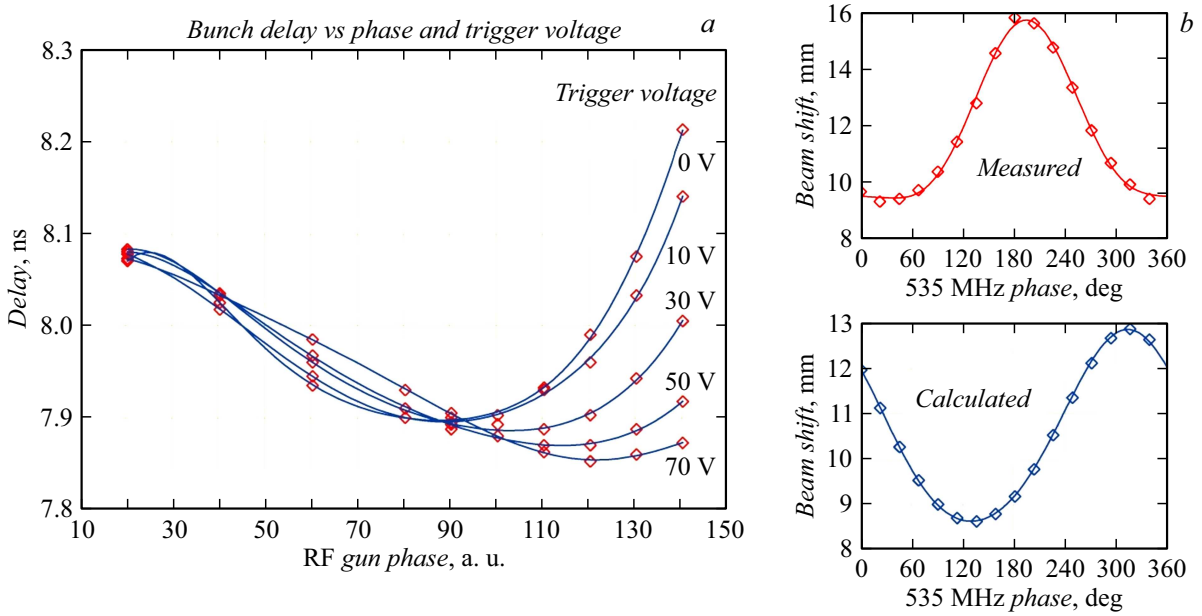

Figure 8. Dependences of bunch passage delays on the phase of the RF gun and bias voltage of the cathode (a) and deviation in the correcting coil when calibrating the phase of the cavity 535.5 MHz for the bias voltage 0 V and operating phase of the RF gun 40° (0.3 nC) (b).

which correspond to the maximum energy of particles and are compared to estimated delays (τ), obtained from the relativistic dependence of speed $\beta = v/c$ on particle energy $\mathscr{E}$:

$$\beta = \sqrt{1 - \frac{1}{(1 + \mathscr{E}/mc^2)^2}},$$

where m — electron mass, c — light velocity, $\mathscr{E}$ — particle energy set by the AGC system.

The measured delay between pulses on the oscilloscope is equal to the sum of bunch delays between FCT1, FCT2 sensors separated by distance S and in cables with length difference L:

$$\tau = \frac{S}{\beta c} + \frac{L}{c/1.52}. \qquad (2)$$

Therefore, the delay is determined by three parameters: K, S, L. All three parameters (Table 2) were found by the least-square method for the difference of measured delays with the ones calculated using equation (2). In Fig. 7, b the measured dependence of delays is shown with a red curve (Delay), and the difference between the measured curve and the calculated one is shown as a brown curve (Difference — the right scale in picoseconds). From the curve it follows that rms accuracy of this precision is 0.02%.

During calibration, the oscilloscope by ROHDE-SCHWARZ with band 4 GHz and sampling rate 20 GSampl/s was used. Each measurement was averaged by 10 impulses. Limitation of the frequency band causes specific distortion of the edge of impulses from FCT sensors that also have their limited band. Fig. 6, b shows as an example the result of limiting the spectrum

Table 2. Results of RF gun voltage calibration

K, keV/V	S, m	L, m
99.81952	2.12504	0.0229

of frequencies as broken down into Fourier series for the estimated current pulse in the bunch. Such resulting shape of the pulse complies with the typical images from the oscilloscope screen (Fig. 7, c). It shows a dip wave with positive values on the front edge (on the curve of Fig. 7, c the signal from electron bunches is negative) and accelerating in the tail portion. During calibration, the time of edge arrival was measured at half maximum between the positive levels of the dip wave and pulse minima. This approach demonstrated good accuracy of measurements in practice. By the way, limitation of the pulse spectrum does not cause changes to the integral value from the current pulse in time, i. e. pulse charge. Therefore, when measuring the charge (Fig. 6) all values of the measured pulse shape were integrated together with dips.

3.3. Calibration of phase of third harmonic cavity (535.5 MHz)

Calibration of the third harmonic cavity phase must be carried out individually for each operating phase of the RF gun and the operating trigger voltage of the cathode in it (for charge in the bunch 0.3 or 1 nC). It is related to the fact that the time of bunch exit from the RF gun or their exit phase depend on these parameters, as follows from Fig. 8, a. Fig. 8, a shows the results of

measurements of the time of bunches passage between two FCT sensors depending on the phase of the RF gun and trigger voltage of the cathode. This dependence, as the dependence of the phase in the maximum of charge on the trigger voltage, arises according to the above reasons.

During calibration the measurement of the transverse deviation of bunches was used in the corrector (with fixed deflecting field) due to the variable energy of bunches when the phase of the cavity 535.5 MHz varies. Bunch energy varies within ± 150 keV while the phase varies from 0 to 360°. The obtained dependence (as the estimated one) is interpolated by first two members of the Fourier series and is compared to the estimated one. From the comparison of these two dependences, the calibration phase shift is calculated, where the phase is set on the panel. Fig. 8, *b* shows the results of calibration for one of the grouping modes of the preinjector (Fig. 5), from which it follows that the phases from the panel (a.u.) must be adjusted by the value of the shift 116.4, in order to obtain the real phases in degrees of RF 535.5 MHz, corresponding to the moment of bunch center exit from the cathode.

Conclusion

The paper analyzes the dynamics of the beam in the preinjector with the thermionic cathode RF gun for SKIF fourth generation synchrotron. A brief review is given for the globally existing thermionic cathode RF guns, their properties and features of operation are specified. Advantages of using the thermionic cathode RF gun are described with the grid control. The description and design of the preinjector with the RF gun are provided, as well as the principle of bunch grouping on the basis of the preinjector RF system. Differences and features of operation of this preinjector are analyzed compared to the similar injectors based on static guns. Results of numerical calculations and experimental data of the bunch grouping process and features of the beam interaction with the RF system are provided. The algorithm is developed for tuning the grouping system. It is shown that 100% passage will not yet guarantee the nominal 1% energy spread in the beam. For precision tuning it is necessary to periodically calibrate the RF system, which must be automated to the maximum. Methods are developed to calibrate amplitudes and phases of the RF gun and buncher cavity.

Conflict of interest

The authors declare that they have no conflict of interest.

References

[1] S.M. Gurov, V.N. Volkov, K.V. Zolotarev, A.E. Levichev. J. Surf. Investigation: X-ray, Synchrotron and Neutron Techniques, **14** (4), 651 (2020).

[2] C. Christou, V. Kempson, K. Dunkel, C. Piel. *The Preinjector Linac for the Diamond Light Source, Proceed. of LINAC* (Lübeck, Germany, 2004), p. 84–86.

[3] M. Pedrozzi, M. Dehler, P. Marchand, L. Rivkin, V. Schlott, A. Streun, C. Piel. *Commissioning of the SLS linac, EPAC 2000* (Vienna, 2000), p. 851.

[4] T. Shaftan, A. Blednykh, E. Blum, W. Cheng, J. Choi, B. Dalesio, M. Davidsaver, J. De Long, R. Fliller, M. Johanson, F. Gao, W. Guo, G. Ganetis, A. Goel, K. Ha, R. Heese, H.-C. Hseuh, S. Kramer, B. Kosciuk, S. Kowalski, Y. Li, W. Louie, S. Ozaki, D. Padrazo, J. Rose, S. Seletskiy, S. Sharma, B. Singh, O. Singh, V. Smaluk, G. Shen, Y. Tian, K. Vetter, W. Wahl, G. Wang, F. Willeke, X. Yang, L.H. Yu, E. Zitvogel, P. Zuhoski. *Status of NSLS-II injector, Proceed. of IPAC 2013* (Shanghai, China, 2013), p. 273–275.

[5] T. Perron, E. Rabeuf, E. Plouviez, V. Serriere, A. Panzarella, B. Ogier. *New Preinjector for the ESRF Booster, Proceed. of EPAC08* (Genoa, Italy, 2008), p. 2195–2197.

[6] B. Taylor, H. Lancaster, H. Hoag. *Engineering Design of the Injector Linac for the Advanced Light Source (ALS), Proceed. of the 1988 Linear Accelerator Conference* (Williamsburg, Virginia, USA), p. 565–567.

[7] X.C. Ma, M.V. Arsentyeva, E.A. Bekhtenev, V.G. Cheskidov, V.M. Borin, G.V. Karpov, Y.I. Maltseva, O.I. Meshkov, D.A. Nikiforov, O.A. Pavlov, V. Volkov. *Beam Instrumentation for Linear Accelerator of SKIF Synchrotron Light Source, IPAC 2021, Proceed. of the 12th International Particle Accelerator Conference* (Campinas, SP, Brazil : JACoW, 2021),p. 1016–1019.
DOI: 10.18429/JACoW-IPAC2021-MOPAB328

[8] S. Ma, M.V. Arsenieva, A.M. Batrakov, A.E. Levichev, V.N. Volkov, O.I. Meshkov, Yu.I. Maltseva, D.A. Nikiforov, A.v. Pavlenko, Kuanjun Fan. Sibirskiy fizicheskiy zhurnal, **18** (1), 14 (2023) (in Russian).
DOI: 10.25205/2541-9447-2023-18-1-14-27

[9] V.N. Volkov, V.S. Arbuzov, E.K. Kenzhebulatov, E.I. Kolobanov, A.A. Kondakov, E.V. Kozyrev, S.A. Krutikhin, G.Ya. Kurkin, I.V. Kuptsov, S.V. Motygin, A.A. Murasev, V.K. Ovchar, V.M. Petrov, A.M. Pilan, V.V. Repkov, I.K. Sedlyarov, S.S. Serednykov, O.A. Shevchenko, M.A. Sheglov, S.V. Tararyshkin, A.G. Tribendis, N.A. Vinokurov. *Test Stand Results of CW 100 mA RF gun for Novosibirsk ERL based FEL* in Proc. *RuPAC.18* (Protvino, Russia, 2018), p. 507–509.

[10] V.N. Volkov, V.S. Arbuzov, K.N. Chernov, E.I. Kolobanov, S.A. Krutikhin, G.Ya. Kurkin, E.A. Kuper, I.V. Kuptsov, S.V. Motygin, V.N. Osipov, V.K. Ovchar, V.V. Repkov, V.M. Petrov, I.K. Sedlyarov, G.V. Serdobintzev, S.S. Serednjakov, M.A. Scheglov, S.V. Tararyshkin, A.G. Tribendis, I.A. Zapryagaev, I.V. Shorikov, A.V. Telnov, N.V. Zavyalov. *CW 100 keV Electron RF Injector for 40 mA Average Beam Current, Proceed. of RuPAC 2014* (Obninsk, 2014), p. 309–311.

[11] P. Sprangle, J. Penano, B. Hafizi, D. Gordon, S. Gold, A. Ting, C. Mitchell. Phys. Rev. Special Topics — Accelerators and Beams, **14**, 020702 (2011).

[12] M. Borland. *A High-Brightness Thermionic Microwave Electron gun* (SLAC-402, UC-41 4, (A), February 1991, Ph.D. Thesis)
[13] V.L. Auslender, V.V. Bezuglov, A.A. Bryazgin, V.A. Gorbunov, V.G. Cheskidov, I.V. Gornakov, B.L. Faktorovich, V.E. Nekhaev, V.S. Podobaev, A.D. Panfilov, A.V. Sidorov, V.O. Tkachenko, A.F. Tuvik, L.A. Voronin. *Industrial Electron Accelerators Type ILU, Proceed. of RuPAC 2006* (Novosibirsk, Russia, 2006), p. 351–353.
[14] K. Floettmann. *ASTRA User's Manual*, http://www.desy.de mpyflo/Astra_dokumentation
[15] V. Volkov, E. Kenjebulatov, S. Krutikhin, G. Kurkin, V. Petrov, E. Rotov, N. Vinokurov. *Thermionic Cathode-Grid Assembly Simulations for rf Guns* (Budker Institute of Nuclear Physics, Novosibirsk, Russia, PAC09, Vancouver, Canada, 4–8 May, 2009), p. 572–574.
[16] D.G. Myakishev, V.P. Yakovlev. *CLANC2-A Code for Calculation of Multipole Modes in Axisymmetric Cavities with Absorber Ferrites*, Proceed. of the Particle Accelerator Conference (NY., 1999), p. 2775–2777.
[17] *CST Studio Suite Electromagnetic Field Simulation Software*: URL: https://www.3ds.com/products-services/simulia/products/cst-studio-suite/
[18] A. Levichev, K. Grishina, S. Samoilov, M. Arsentieva, D. Chekmenev, Ma Xiaochao, O. Meshkov, I. Pivovarov, D. Nikiforov, A. Barnyakov. J. Instrumentation, 18, T07001 (2023). DOI: 10.1088/1748-0221/18/07/T07001
[19] V.N. Volkov, M.V. Arsenieva, A.M. Barnyakov, A.M. Batrakov, E.A. Bekhtenev, N.G. Vasilieva, S.M. Gurov, S.E. Karnaev, A.A. Kondakov, A.N. Kosarev, S.A. Krutikhin, G.Ya. Kurkin, A.E. Levichev, A.Yu. Martynovsky, S.V. Motygin, D.A. Nikiforov, V.K. Ovchar, A.V. Pavlenko, O.A. Pavlov, M.V. Rodyakin, E.A. Rotov, I.K. Sedlyarov, A.M. Sememov, M.G. Fedotov, K.N. Chernov. ZhTF, **94** (6), (2024) (in Russian).

Translated by M.Verenikina